

Theoretical Studies on the Local Structure and Electron Paramagnetic Resonance Parameters for Cu^{2+} Centers in TiO_2 with one Oxygen Vacancy Adjacent

Chao-Ying Li, Xue-Mei Zheng, and Jie He

School of Physics and Electronic Information, Shangrao Normal University, Shangrao Jiangxi 334000, P. R. China

Reprint requests to C.-Y. L.; E-mail: cyl1962@gmail.com

Z. Naturforsch. **68a**, 605–609 (2013) / DOI: 10.5560/ZNA.2013-0035

Received November 26, 2012 / revised April 9, 2013 / published online June 12, 2013

Based on the defect model that the impurity Cu^{2+} in TiO_2 on the octahedral Ti^{4+} site is associated with one oxygen vacancy V_O along the C_2 axis, the electron paramagnetic resonance (EPR) parameters, i. e., the g factors g_i ($i = x, y, z$) and the hyperfine structure constants A_i , of the $\text{Cu}^{2+}-\text{V}_\text{O}$ center in TiO_2 are calculated by using the perturbation formulas of these parameters for a $3d^9$ ion in a rhombically elongated octahedra. From this study, the impurity Cu^{2+} is found to be away from V_O by a distance Δz ($\approx 0.33 \text{ \AA}$) along the C_2 axis, meanwhile the four O^{2-} ions in the plane perpendicular to the C_2 axis may be shifted by Δx ($\approx 0.28 \text{ \AA}$) towards V_O due to the electrostatic interaction between these ions and V_O . The theoretical results based on the above local structure distortions show good agreement with the experimental data.

Key words: Electron Paramagnetic Resonance (EPR); Defect Structures; Cu^{2+} ; Oxygen Vacancies (V_O); TiO_2 .

1. Introduction

When doped with transition metal ions, TiO_2 exhibits interesting photocatalysis [1, 2] and magnetic and electronic structural properties [3–6]. These properties or behaviours are usually related to the electronic and structural properties of the doped ions in this material. Since the electron paramagnetic resonance (EPR) technique is a powerful tool to study defect structures of paramagnetic impurities in crystals, extensive studies have been carried out on the defect structures and interactions between impurity and ligands for some transition-metal ions (i. e., Cu^{2+} , Fe^{3+} , Mn^{2+} , Co^{2+}) doped TiO_2 by analyzing their EPR data [7–10]. Decades ago, the EPR spectra of Cu^{2+} -doped TiO_2 crystals were measured [11] and attributed to the impurity Cu^{2+} occupying the 6-fold coordinated octahedral Ti^{4+} site with no charge compensation despite charge mismatch between the host Ti^{4+} and the impurity Cu^{2+} . The EPR parameters and the local lattice distortion for this Cu^{2+} center were also investigated [7, 12]. Whereas, recently, Brant et al. proposed a new model for the impurity Cu^{2+} doped in TiO_2

crystals, they suggested that the impurity Cu^{2+} is at the 5-fold coordinated octahedral Ti^{4+} site associated with one oxygen vacancy V_O along the C_2 axis forming the $\text{Cu}^{2+}-\text{V}_\text{O}$ center due to the charge compensation (see Fig. 1). The EPR parameters (the anisotropic g factors g_i ($i = x, y, z$) and the hyperfine structure constants A_i) were also measured [13]. However, no theoretical explanations for the above Cu^{2+} centers in TiO_2 have been made until now.

In view of that information about local structures and electronic states for the Cu^{2+} centers in TiO_2 , it would be helpful to understand the microscopic mechanisms of EPR behaviours for these materials containing Cu^{2+} dopants. Further investigations on the EPR parameters and defect structures for these Cu^{2+} centers are of fundamental and practical significance. In this work, the perturbation formulas of the EPR parameters for a Cu^{2+} ($3d^9$) ion under rhombically elongated octahedral are adopted, including the reasonable local lattice distortion (i. e., the impurity displacement Δz along the C_2 axes and the ligand shift Δx towards V_O) due to the electrostatic interaction between these ions and V_O (see Fig. 2).

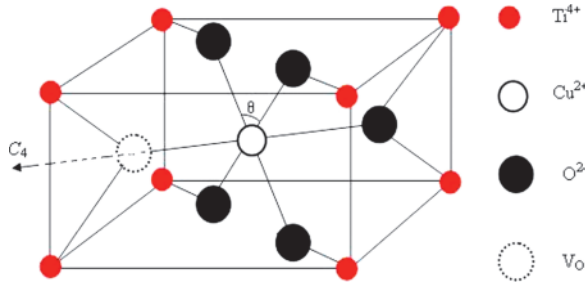


Fig. 1 (colour online). TiO_2 (rutile) crystal structure showing a TiO_6 unit: a Cu^{2+} ion substitutes for a Ti^{4+} ion and has an oxygen vacancy along the C_4 axis.

2. Calculations

In the TiO_2 (rutile structure) crystal, the Ti^{4+} ion is coordinated to a slightly elongated oxygen octahedron with two longer bond lengths R_{\parallel} ($\approx 1.988 \text{ \AA}$ [14]) parallel to the C_2 axis and four coplanar shorter bond lengths R_{\perp} ($\approx 1.944 \text{ \AA}$ [14]) perpendicular to the axis with the axial distortion angle $\alpha \approx \tan^{-1}(R_{\perp}/R_{\parallel})$. In addition, the planar bond angle θ ($\approx 80.88^\circ$ [14]) inducing the rhombic distortion (i. e., $\delta\theta = \theta_0 - \theta$ where $\theta_0 = 90^\circ$ is the value for an ideal octahedron). When the impurity Cu^{2+} is doped into the lattice of TiO_2 , it may replace the host Ti^{4+} . However, since Cu^{2+} has less charge as compared with the replaced Ti^{4+} , one nearest neighbour oxygen vacancy V_{O} may occur along the C_2 axis as compensator [13]. Accordingly, the Cu^{2+} ion impurity may be displaced away from the center of the octahedron by an amount Δz along the C_2 axis, meanwhile the four O^{2-} ion ligands in the plane perpendicular to the C_2 axis may be shifted by a certain displacement Δx towards V_{O} due to the electrostatic interaction between these ions and V_{O} .

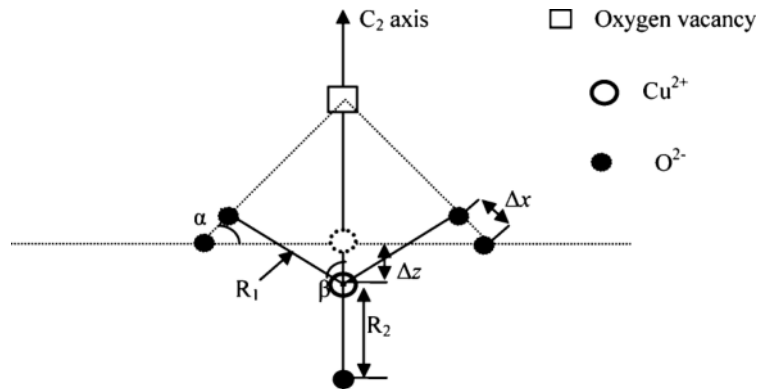


Fig. 2. Projective view of the impurity Cu^{2+} center in a TiO_2 crystal with one oxygen vacancy adjacent along the C_2 axis.

For a $3d^9$ (Cu^{2+}) ion in rhombically elongated octahedra, its lower orbital doublet 2E_g would be separated into two singlets ${}^2A_{1g}(\theta)$ and ${}^2A'_{1g}(\epsilon)$ with the latter lying lowest. Meanwhile, the higher cubic orbital triplet ${}^2T_{2g}$ would be split into three singlets ${}^2B_{1g}(\zeta)$, ${}^2B_{2g}(\eta)$, and ${}^2B_{3g}(\xi)$ [15]. For the studied $[\text{CuO}_5]^{8-}$ octahedral cluster, since the charge-transfer (CT) energy levels are much higher than the crystal-field (CF) energy levels, the contributions of the CT mechanism to the EPR parameters can be neglected. Because the studied $\text{TiO}_2 : \text{Cu}^{2+}$ has insignificant covalency and weak ligand spin-orbit coupling interaction, the formulas based on the conventional CF model are reasonably adopted here for simplicity, considering merely the contributions from the central ion orbitals and spin-orbit coupling interaction. Thus, we have [12, 16]:

$$\begin{aligned}
 g_x = & g_s + 2k\zeta/E_2 + k\zeta^2 \left[(2/E_1 - 1/E_3)/E_2 - 4/(E_1E_3) \right] \\
 & + g_s\zeta^2 \left[2/E_1^2 - (1/E_2^2 - 1/E_3^2)/2 \right] - k\zeta^3 \\
 & \cdot \left\{ (1/E_2 - 1/E_3)(1/E_3 + 1/E_2)/(2E_1) + (2/E_1 \right. \\
 & \left. - 1/E_2)(2/E_1 + 1/E_2)/2E_3 - (1/E_2 - 1/E_3)/(2E_2E_4) \right\} \\
 & + (g_s\zeta^3/4) \left[(1/E_3 - 2/E_1)/E_2^2 + (2/E_3 - 1/E_2)/E_3^2 \right. \\
 & \left. + 2(1/E_2 - 1/E_3)/E_1^2 + 2(1/E_2^2 - 1/E_3^2)/E_1 \right], \\
 g_y = & g_s + 2k\zeta/E_3 + k\zeta^2 \left[(2/E_1 - 1/E_2)/E_3 - 4/(E_1E_2) \right] \\
 & + g_s\zeta^2 \left[2/E_1^2 - (1/E_3^2 - 1/E_2^2)/2 \right] + k\zeta^3 \\
 & \cdot \left\{ (1/E_2 - 1/E_3)(1/E_3 + 1/E_2)/(2E_1) + (2/E_1 \right. \\
 & \left. - 1/E_3)(2/E_1 + 1/E_3)/2E_2 - (1/E_3 - 1/E_2)/(2E_3E_4) \right\} \\
 & + (g_s\zeta^3/4) \left[(1/E_2 - 2/E_1)/E_3^2 + (2/E_2 - 1/E_3)/E_2^2 \right]
 \end{aligned}$$

$$\begin{aligned}
& + 2(1/E_3 - 1/E_2)/E_1^2 + 2(1/E_3^2 - 1/E_2^2)/E_1, \quad (1) \\
g_z = & g_s + 8k\zeta/E_1 + k\zeta^2 \left[1/(E_3E_2) + 2(1/E_1E_2 \right. \\
& \left. + 1/E_1E_3) \right] - g_s\zeta^2 \left[1/E_1^2 - (1/E_2^2 + 1/E_3^2)/4 \right] \\
& + k\zeta^3 \left[8/E_1 - (1/E_2 + 1/E_3) \right] / (2E_2E_3) - 2k\zeta^3 \\
& \cdot \left[1/(E_1E_2) + 1/(E_1E_3) - 1/(E_2E_3) \right] / E_1 + (g_s\zeta^3/4) \\
& \cdot \left[2(1/E_2^2 + 1/E_3^2)/E_1 - (1/E_2 + 1/E_3)/(E_2E_3) \right], \\
A_x = & P \left[-\kappa - \kappa' + 2N/7 + 11(g_x - g_s)/14 \right], \\
A_y = & P \left[-\kappa + \kappa' + 2N/7 + 11(g_y - g_s)/14 \right], \\
A_z = & P \left[-\kappa - 4N/7 + (g_z - g_s) + 3(g_x + g_y - 2g_s)/7 \right].
\end{aligned}$$

Here g_s (≈ 2.0023) is the spin-only value, and k is the orbital reduction factor. ζ and P are, respectively, the spin-orbit coupling coefficient and the dipolar hyperfine structure parameter for the $3d^9$ ion in crystals. κ is the isotropic core polarization constant and κ' the anisotropic one due to the rhombic distortion of the Cu^{2+} center. For a $3d^n$ ion in crystals with weak covalence, the average covalence reduction factor N is introduced to characterize the covalence reduction effect [17]; thus we have

$$\zeta \approx N\zeta_0, \quad P \approx N^2P_0, \quad k \approx N. \quad (2)$$

The denominators E_i ($i = 1-4$) denote, respectively, the energy separations between the excited ${}^2A_{1g}(\theta)$, ${}^2B_{1g}(\zeta)$, ${}^2B_{2g}(\eta)$, and ${}^2B_{3g}(\xi)$ and the ground ${}^2A_{1g}(\varepsilon)$ states. They are determined from the energy matrix for a $3d^9$ ion under rhombic symmetry in terms of the cubic field parameter D_q and the rhombic field parameters D_s , D_t , D_ξ , and D_η :

$$\begin{aligned}
E_1 & \approx 4D_s + 5D_t, \\
E_2 & \approx 10D_q, \\
E_3 & \approx 10D_q - 3D_s + 5D_t + 3D_\xi - 4D_\eta, \\
E_4 & \approx 10D_q + D_s + 10D_t - 3D_\xi + 4D_\eta.
\end{aligned} \quad (3)$$

For the studied Cu^{2+} center in the octahedral $[\text{CuO}_5]^{8-}$ cluster, the five ligands are divided into two parts, i.e., the four planar ones with bond lengths R_1 and one with bond length R_2 due to the impurity displacement Δz along the C_2 axis and the shift Δx of the planar ligands towards V_O . The angle between the planar bond length R_1 and the C_2 axis is defined as β . Thus, the local bond lengths and bond angle are determined as (see Fig. 1)

$$\begin{aligned}
R_1 & \approx \left[(R_\perp - \Delta x \cos \alpha)^2 + (\Delta z + \Delta x \sin \alpha)^2 \right]^{1/2}, \\
R_2 & \approx R_\parallel - \Delta z, \\
\cos \beta & \approx (\Delta z + \Delta x \sin \alpha) / R_1.
\end{aligned} \quad (4)$$

From the local geometry and the superposition model [18], the related rhombic crystal-field parameters can be expressed as

$$\begin{aligned}
D_s & \approx (2/7)\bar{A}_2(R_0) \left[2(3 \cos^2 \beta - 1)(R_0/R_1)^{t_2} \right. \\
& \left. + (R_0/R_2)^{t_2} \right], \\
D_t & \approx (4/21)\bar{A}_4(R_0) \left[(35 \cos^4 \beta - 30 \cos^2 \beta + 3 \right. \\
& \left. - 7 \sin^4 \beta)(R_0/R_1)^{t_4} + 2(R_0/R_2)^{t_4} \right], \quad (5) \\
D_\xi & \approx (2/7)\bar{A}_2(R_0) \left[\sin^2 \beta (R_0/R_2)^{t_2} \right] \cos \theta, \\
D_\eta & \approx (20/21)\bar{A}_4(R_0) \left[\sin^2 \beta (7 \cos^2 \beta \right. \\
& \left. - 1)(R_0/R_1)^{t_4} \right] \cos \theta.
\end{aligned}$$

Here $t_2 \approx 3$ and $t_4 \approx 5$ are the power-law exponents due to the dominant ionic nature of the bonds [19, 20]. $\bar{A}_2(R_0)$ and $\bar{A}_4(R_0)$ are the intrinsic parameters with the reference distance R_0 ($\approx 1.959 \text{ \AA}$), which is the metal-ligand distance related to the octahedral Ti^{4+} site in the host TiO_2 crystal [14]. The ratio $\bar{A}_2(R_0)/\bar{A}_4(R_0)$ is in the range of 9 ~ 12 [12, 21–23]; we take $\bar{A}_2(R_0) \approx 9\bar{A}_4(R_0)$ here. For $3d^n$ ions in octahedral clusters, the relationship $\bar{A}_4(R_0) \approx (3/4)D_q$ [21] is held for many systems, where D_q is the cubic field parameter of the studied system. Since no optical spectral data

Table 1. g factors g_i ($i = x, y, z$) and hyperfine structure constants A_i (in 10^{-4} cm^{-1}) for $\text{TiO}_2 : \text{Cu}^{2+}$ with one oxygen vacancy adjacent along the C_4 axis.

	g_x	g_y	g_z	${}^{63}A_x$	${}^{63}A_y$	${}^{63}A_z$	${}^{65}A_x$	${}^{65}A_y$	${}^{65}A_z$
Cal.	2.1056	2.0915	2.3471	18.18	25.83	-82.77	19.50	27.69	-88.74
Exp. [13]	2.10699	2.09281	2.34518	18.46	27.47	-87.39	19.75	29.42	-93.67

of TiO₂ : Cu²⁺ were reported, the spectral parameters $D_q \approx 1350 \text{ cm}^{-1}$ and $N \approx 0.83$ can be obtained from the optical spectral studies for Cu²⁺ in KTaO₃ and some oxides [21, 24]. Then the spin-orbit coupling coefficient ζ for TiO₂ : Cu²⁺ is acquired as the free-ion value ζ_0 ($\approx 829 \text{ cm}^{-1}$ [15, 21]) multiplying N .

Thus, in the above formulas for the g factors in (1), there are only two unknown parameters, i. e., the impurity displacement Δz and the planar ligand shift Δx towards V_O for the studied Cu²⁺ center in TiO₂. Substituting the related values into (1) and fitting the theoretical results to the experimental data, one gets

$$\Delta z \approx 0.33 \text{ \AA} \text{ and } \Delta x \approx 0.28 \text{ \AA}. \quad (6)$$

From these values, the local structure parameters can be obtained, i. e., $R_1 \approx 1.828 \text{ \AA}$, $R_2 \approx 1.624 \text{ \AA}$. The calculated g factors are compared with the experimental values in Table 1.

In the formulas of the hyperfine structure constants, the dipolar hyperfine structure parameters P_0 are $388 \cdot 10^{-4} \text{ cm}^{-1}$ and $416 \cdot 10^{-4} \text{ cm}^{-1}$ for the free ⁶³Cu and ⁶⁵Cu [25], respectively. The core polarization constant can be determined from the relationship $\kappa \approx -2\chi/(3\langle r^{-3} \rangle)$, where χ is characteristic of the density of unpaired spins at the nucleus of the central ion, and $\langle r^{-3} \rangle$ is the expectation value of the inverse cube of the 3d radial wave function. From the data $\langle r^{-3} \rangle \approx 8.25 \text{ a. u.}$ [15] and $\chi \approx -3.40 \text{ a. u.}$ [25] for Cu²⁺ in TiO₂, one can obtain $\kappa \approx 0.23$. Substituting the above parameters into (1) and fitting the calculated A factors to the observed values, the anisotropic core polarization constant can be obtained, i. e.,

$$\kappa' \approx 0.02. \quad (7)$$

3. Discussion

According to Table 1, one can find that the calculated g factors g_i and the hyperfine structure constants A_i based on the above local lattice distortion agree reasonably with the experimental data. Thus the observed EPR results are interpreted in this work, and the defect structure (i. e., Cu²⁺-V_O) model proposed in [13] of TiO₂ : Cu²⁺ is also confirmed.

(i) The signs of Δz (and Δx) > 0 show that the displacement direction of the Cu²⁺ ion impurity and that of the O²⁻ ion ligands in the studied [CuO₅]⁸⁻ cluster are consistent with the expectation based on the electrostatic interaction between these ions and V_O. Moreover, due to the relatively larger distance between V_O

and the four O²⁻ ions in the plane perpendicular to the C₂ axis compared to R₂ for the impurity Cu²⁺ ion, the obtained Δz ($\approx 0.33 \text{ \AA}$) being slightly larger than Δx ($\approx 0.28 \text{ \AA}$) from the analysis of the EPR parameters is physically reasonable. Interestingly, similar impurity displacements Δz ($\approx 0.2 \sim 0.3 \text{ \AA}$) due to the apical V_O were also reported for various transition-metal ions (e. g., Co²⁺, Cu²⁺, Fe³⁺, Ni³⁺) on the octahedral Ta⁵⁺ (or Nb⁵⁺) site in KTaO₃ (or KNbO₃) based on the EPR analysis [21, 26–29], shell-model simulations, and embedded-cluster calculations [30].

(ii) From (1), the hyperfine structure constants A_i ($i = x, y, z$) originate mainly from the isotropic contributions proportional to the core polarization constant κ , characteristic of the Fermi contact between the ground 3s²3d⁹ configuration and the excited s-orbitals (e. g., 3s¹3d⁹4s¹) for the central ion in crystals. The anisotropy parts of the A factors are mainly related to the covalency factor N and the g shifts ($= g_i - g_s$, $i = x, y$, and z), which are somewhat relevant to the local structure (rhombical distortion) of the impurity center. However, the small optimal anisotropic core polarization constants κ' (≈ 0.02 , which are much smaller than the isotropic $\kappa \approx 0.23$) and the g anisotropies δg ($= g_x - g_y$) attribute some anisotropic contributions δA ($= A_x - A_y$) for the A factors.

(iii) Unlike the studied Cu²⁺ center on Ti⁴⁺ site in [7, 12] without charge compensation, the studied impurity center in this work is Cu²⁺ at the 5-fold coordinated octahedral Ti⁴⁺ site associated with one oxygen vacancy V_O along the C₂ axis. The above different local structures for Cu²⁺ in TiO₂ may be attributed to the different experimental preparation conditions. This point is also supported by the cubic field parameter D_q ($\approx 1350 \text{ cm}^{-1}$) obtained for the Cu²⁺-V_O center (i. e., [CuO₅]⁸⁻ cluster) from the optical spectral analysis in [21], which is about 12% smaller than that ($\approx 1540 \text{ cm}^{-1}$ [12]) for Cu²⁺ in TiO₂ with no charge compensation (i. e., [CuO₆]¹⁰⁻ clusters). Interestingly, one and two oxygen vacancies V_O were reported for the [CuO₅]⁸⁻ and [CuO₄]⁶⁻ clusters at the Ta⁵⁺ site in Cu²⁺ doped KTaO₃ due to charge compensation [21].

(iv) There are some errors in the above calculations. First, the approximation of the theoretical model and the formulas can induce some errors for the resultant EPR parameters and the local structural parameters Δz and Δx . Second, it should be pointed out that the above calculations are based on the crystal-field theory, the

contributions of the spin–orbit coupling coefficient of the ligands as well as the ligand p and s orbitals are ignored. Fortunately, for the studied $[\text{CuO}_5]^{8-}$ cluster, the above contributions can be regarded as negligible because of the much smaller spin–orbit coupling coefficient ($\approx 151 \text{ cm}^{-1}$ [10]) of the ligand oxygen than that ($\approx 829 \text{ cm}^{-1}$ [15]) of the central Cu^{2+} . Third, the errors of the local structure and the EPR parameters also arise from the approximation of the relationship $\bar{A}_2(R_0) \approx 9\bar{A}_4(R_0)$, which would somewhat affect the rhombic field parameters (4) and the final results. According to the calculations, the errors in the final EPR parameters and the local structural parameters are estimated to be not more than 1% when the ratio $\bar{A}_2(R_0)/\bar{A}_4(R_0)$ varies by 10%. Finally, the contributions of the still higher (fifth) order perturbation terms in the formulas for the g factors in (1) was

not considered. However, the crude estimation of the higher (fifth) order perturbation term $\zeta^4/(E_1^3 E_2)$ is in the order of 10^{-6} and safely negligible.

4. Conclusions

The EPR parameters and the local structure for the Cu^{2+} centre in TiO_2 with one oxygen vacancy along the C_2 axis are theoretically investigated from the perturbation formulas for a $3d^9$ ion in rhombically elongated octahedra. The impurity Cu^{2+} experiences an off-center displacement Δz ($\approx 0.33 \text{ \AA}$) away from V_O along the C_2 axis. Additionally, the four O^{2-} ions in the plane perpendicular to the C_2 axis may shift by an amount Δx ($\approx 0.28 \text{ \AA}$) towards V_O due to the electrostatic interaction between these ions and V_O .

- [1] J. Zhu, F. Chen, J. Zhang, H. Chen, and M. Anpo, *J. Photochem. Photobiol. A* **180**, 196 (2006).
- [2] M. Iwasaki, M. Hara, H. Kawada, H. Tada, and S. Ito, *J. Colloid Interf. Sci.* **224**, 202 (2000).
- [3] M. M. Islam, T. Bredow, and A. Gerson, *Chem. Phys. Chem.* **12**, 3467 (2011).
- [4] Y. J. Lee, M. P. de Jong, and W. G. van der Wiel, *Phys. Rev. B* **83**, 134404 (2011).
- [5] R. Asahi, Y. Taga, W. Mannstadt, and A. J. Freeman, *Phys. Rev. B* **61**, 7459 (2000).
- [6] K. M. Glassford, N. Troullier, J. Martins, and J. R. Chelikowsky, *Solid State Commun.* **76**, 635 (1990).
- [7] H. N. Dong, S. Y. Wu, and P. Li, *Phys. Status Solidi B* **241**, 1935 (2004).
- [8] J. Z. Lin, *Braz. J. Phys.* **40**, 344 (2010).
- [9] S. Y. Wu and W. C. Zheng, *Z. Naturforsch.* **57a**, 45 (2002).
- [10] W. Y. Tian, X. Y. Kuang, M. L. Duan, R. P. Chai, and C. X. Zhang, *Physica B* **404**, 4332 (2009).
- [11] T. C. Ensign, T. T. Chang, and A. H. Kahn, *Phys. Rev.* **188**, 703 (1969).
- [12] H. M. Zhang, S. Y. Wu, P. Xu, and L. L. Li, *Mod. Phys. Lett. B* **24**, 2357 (2010).
- [13] A. T. Brant, S. Yang, N. C. Giles, M. Z. Iqbal, A. Manivannan, and L. E. Halliburton, *J. Appl. Phys.* **109**, 73711 (2011).
- [14] H. Hikita, K. Takeda, and Y. Kimura, *Phys. Rev. B* **46**, 14381 (1992).
- [15] A. Abragam and B. Bleaney, *Electron Paramagnetic Resonance of Transition Ions*, Oxford University Press, London 1970.
- [16] W. C. Zheng and S. Y. Wu, *Z. Naturforsch.* **55a**, 915 (2000).
- [17] Z. Y. Yang, C. Rudowicz, and J. Qin, *Physica B* **318**, 188 (2002).
- [18] D. J. Newman and B. Ng, *Rep. Prog. Phys.* **52**, 699 (1989).
- [19] H. N. Dong, M. R. Dong, J. J. Li, Q. C. Li, and X. Hong, *J. Chongqing Univ. Posts Telecommun.* **24**, 208 (2012).
- [20] H. M. Zhang, X. Wan, and Z. M. Zhang, *Z. Naturforsch.* **67a**, 407 (2012).
- [21] W. Q. Yang, W. C. Zheng, P. Su, and H. G. Liu, *Cryst. Res. Technol.* **45**, 1132 (2010).
- [22] H. M. Zhang and X. Wan, *J. Non-Cryst. Solids* **43**, 361 (2013).
- [23] Z. H. Zhang, S. Y. Wu, M. Q. Kuang, and X. F. Hu, *Physica B* **408**, 83 (2013).
- [24] A. S. Chakravarty, *Introduction to the Magnetic Properties of Solids*, Wiley-Interscience Publication, New York 1980.
- [25] B. R. McGarvey, *J. Phys. Chem.* **71**, 51 (1967).
- [26] H. N. Dong, *Z. Naturforsch.* **60a**, 615 (2005).
- [27] W. C. Zheng and S. Y. Wu, *Z. Naturforsch.* **57a**, 925 (2002).
- [28] W. C. Zheng and S. Y. Wu, *Appl. Magn. Reson.* **20**, 539 (2001).
- [29] S. Y. Wu, H. N. Dong, and W. H. Wei, *Z. Naturforsch.* **59a**, 203 (2004).
- [30] H. Donnerberg, *Phys. Rev. B* **50**, 9053 (1994).